REVIEW

Medicina (Kaunas) 2013;49(3):97–110

Ischemic Heart Disease: A Comprehensive Evaluation Using Cardiovascular Magnetic Resonance

Tomas Lapinskas

Department of Cardiology, Medical Academy, Lithuanian University of Health Sciences, Lithuania

Key Words: *cardiovascular magnetic resonance; ischemic heart disease; perfusion imaging; myocardial viability; delayed enhancement.*

Summary. *Cardiovascular magnetic resonance is becoming an important imaging modality in clinical cardiology. As an exceptionally accurate and comprehensive diagnostic tool, cardiovascular magnetic resonance is becoming the first-choice modality for imaging the heart and great vessels. Stress cardiovascular magnetic resonance imaging enables the detection of hemodynamically significant coronary artery lesions and the choice of treatment strategy when stenosis is intermediate. Viability assessment is very important as it allows differentiating between dysfunctional but still viable myocardium and predicts the recovery of ventricular function after successful revascularization. However, the availability and costs of cardiovascular magnetic resonance remain the major obstacle and makes the investigation unachievable to many patients.*

Introduction

Cardiovascular magnetic resonance (CMR) is becoming more widely used to assess patients with ischemic heart disease (IHD) and has many substantial advantages over conventional imaging techniques. Recent advances provide a comprehensive evaluation of global and regional ventricular function, myocardial perfusion at rest and during stress, and irreversible myocardial injury using paramagnetic contrast materials in a single study. T2-weighted imaging enables to distinguish acute myocardial damage from chronic. Coronary magnetic resonance angiography (MRA) is rapidly evolving, and recent studies have demonstrated promising results to rule out significant coronary stenosis. CMR is relatively safe, provides high spatial and temporal resolution, and does not expose ionizing radiation, and images can be obtained in any tomographic plane. However, metal implants remain a relevant problem in the magnetic resonance imaging (MRI) system. This review article summarizes a contemporary clinical role of CMR in patients with ischemic heart disease.

Assessment of Ventricular Function

CMR has become a standard of reference for the assessment of global and regional systolic function and the estimation of cardiac volumes and mass. Cine imaging enables the evaluation of ventricular wall motion abnormalities, changes in wall thickness during the cardiac cycle, and accurate assessment of cardiac chamber volumes (1). Balanced steady-state free precession (bSSFP) pulse sequences are most frequently used for functional imaging due to the high contrast differences between intracavitary blood and the myocardium. The conventional cine sequence is a segmented, retrospectively gated acquisition, in which images are obtained during the different phases of the entire cardiac cycle and viewed as a movie. Short-axis cine loops from the mitral valve plane through the apex are acquired with a slice thickness of 6 to 8 mm and a interslice gap of 2 to 4 mm (Fig. 1). These sequences have an in-plane resolution of approximately 1.5 to 2.0 mm^2 and a temporal resolution of 50 ms and less.

Gating is critically important in CMR to avoid the blurring of images. An accurate detection of ECG signal eliminates artifacts caused by the motion of the heart and blood flow. Electric currents produced by the movement of electrically conductive blood though the strong magnetic field distorts the ECG signal. The goal of cardiac synchronization is to obtain a high-amplitude QRS complex, in which R waves are significantly higher than T waves, and the use of vectorcardiography (VCG) improves the detection of R waves. ECG gating can be done either prospectively or retrospectively. The advantage of retrospective gating is the possibility to image the entire cardiac cycle without the loss of the terminal phase of diastole. The respiratory motion causes artifacts in the phase-encoding direction. Fast imaging techniques enables the acquisition of an image during the single breath-hold (10–15 seconds). If gating is unsuccessful, or the patients have an irregular heart rhythm, or cannot hold their breath, real-time imaging may be an alternative (2).

The estimation of ventricular volumes using

Correspondence to T. Lapinskas, Department of Cardiology, Medical Academy, Lithuanian University of Health Sciences, Eivenių 2, 50028 Kaunas, Lithuania
E-mail: tomas.lapinskas@lsmuni.lt

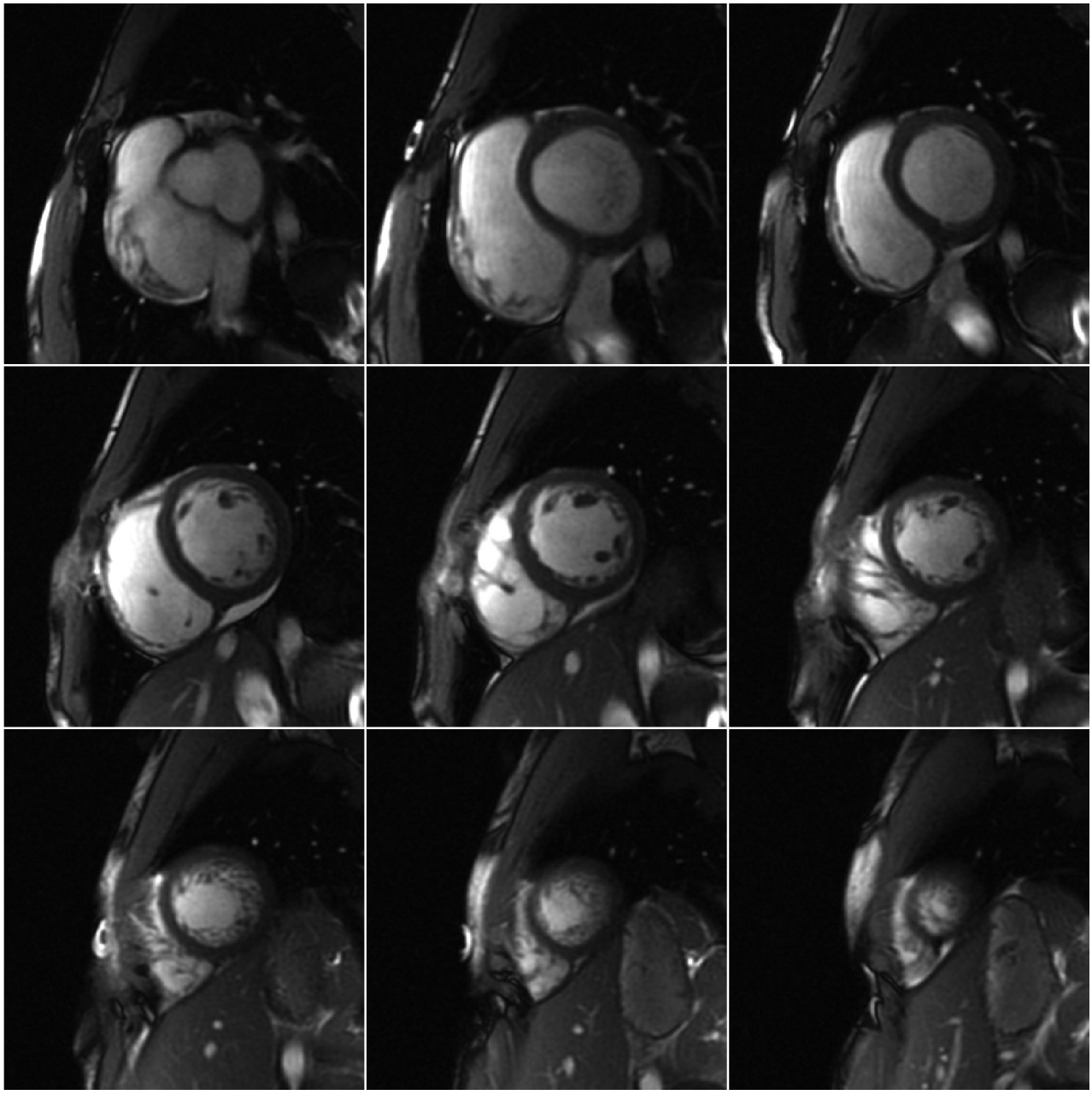


Fig. 1. The stack of short-axis images from the base through the apex at the end-diastolic phase with the slice thickness of 8 mm using a balanced steady-state free precession technique

volumetric methods is more accurate than biplane measurements (3). All short-axis images are assessed with dedicated computer analysis packages for planimetry of endocardial and epicardial contours at ventricular end-diastolic and end-systolic cardiac phases. The major drawback is time required for manual contouring. The calculation of ventricular volumes is based on the disk summation method also known as the modified Simpson's rule. The inclusion or exclusion of the most basal ventricular slice into calculations is associated with a significant variation in the end-diastolic volume. It is recommended to include the most basal slice if 50% or more of the myocardial ring is clearly visible (4). The addition of information on long-axis images improves the identification of the most basal ventricular slice and reduces interstudy variability for all left ventricular functional parameters (5). A 17-segment model proposed by the American College of Cardiology and the American Heart Association is used to assess regional myocardial contraction. Myocardial tagging is the commonly used tissue tracking technique that allows the quantitative assessment of intramyocardial contractile function,

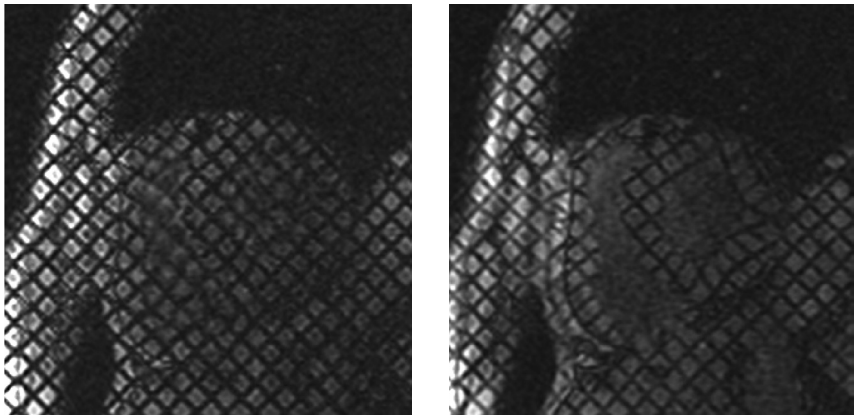


Fig. 2. Myocardial tagging in cardiac short-axis at end-diastolic and end-systolic cardiac phases using spatial modulation of magnetization showing no deformation of tagging grid during ventricular systole in the mid-ventricular anterior, anteroseptal, and inferoseptal segments

strain, and strain rate (Fig. 2). Radiofrequency and gradient pulses saturate tissue magnetization in a linear or grid-like pattern.

CMR is a highly reproducible and accurate imaging modality for the evaluation of ventricular size and function with low intraobserver and interobserver variability (6–11). Echocardiography remains the most widely used noninvasive technique to assess cardiac function. Several studies documented the superiority of CMR over 2-dimensional echocardiography, which is highly operator dependent, often limited by a poor acoustic window, need of geometric assumptions, and less reproducible measurements (3, 12, 13). Even new real-time 3-dimensional echocardiography underestimates left ventricular volumes due to inability to reliably differentiate between the myocardium and trabeculae and is less reproducible than CMR (14).

Ischemia Assessment

Inadequate perfusion of the myocardium causes an imbalance between oxygen supply and demand. The most common cause of myocardial ischemia is obstructive coronary artery disease (CAD). In the absence of segmental atherosclerotic narrowing of epicardial coronary arteries, abnormal constriction or failure of normal vasodilatation of coronary vessels can cause ischemia. Also coronary blood flow may be limited by spasm, arterial thrombi or emboli, congenital abnormalities or inflammation of coronary arteries, or an increase in myocardial oxygen demand. The lack of oxygen during the episodes of inadequate perfusion may cause transient disturbances of the mechanical, biochemical, and electrical functions of the myocardium.

Although several noninvasive imaging modalities are currently available for the evaluation of myocardial ischemia, treadmill or bicycle ergometer exercise testing, stress echocardiography, and stress single-photon emission tomography (SPECT) are most widely used in clinical practice. However, cardiovascular MRI has many advantages over conventional imaging techniques. CMR can accurately assess cardiac morphology, global and regional cardiac function, myocardial ischemia, and viability in the presence of hemodynamically significant coronary lesions in a single session.

Exercise Stress Cardiovascular Magnetic Resonance

Physiologic stress is preferred over pharmacological as it allows not only the detection of myocardial ischemia but also the assessment of individual functional capacity and hemodynamic response (15–17). However, exercise stress CMR is still limited due to the lack of MRI-compatible exercise and monitoring equipment, and exercise stress ECG, echocardiography, or SPECT imaging remain the modalities of choice in the detection, treatment decision-making, and prognosis of cardiovascular diseases (18).

If previously exercise stress CMR was limited due to motion artifacts, the introduction of faster CMR sequences has allowed overcoming these obstacles. Rapid image acquisition after exercise is particularly important and must be completed within 60 seconds to capture exercise-induced wall motion abnormalities (16). However, bringing the exercise and monitoring system inside the MRI environment remains a challenge as it contains of ferromagnetic components. Roest et al. demonstrated the feasibility to perform exercise stress CMR during supine physical exercise stress using an MRI-compatible bicycle ergometer. The investigators evaluated biventricular response to physiologic stress in 16 healthy volunteers. Stroke volume and ejection fraction (EF) increased in both ventricles, end-systolic volumes

of both ventricles decreased from rest to exercise, whereas end-diastolic volumes remained stable (19). Rerkpattanapipat et al. investigated the feasibility of upright treadmill exercise CMR to detect severe coronary stenoses in 27 patients. Ischemia (>70% arterial luminal narrowing) was identified in 14 patients with a sensitivity and specificity of 79% and 85%, respectively (20).

Jekic et al. successfully demonstrated feasibility to perform treadmill stress CMR inside the MRI environment in 20 healthy volunteers. The standard treadmill was modified by replacing all ferromagnetic elements including the components of electromagnetic motor and placed inside the MRI room in a field of 0.2 mT (2 G). After the achievement of exercise limit or the maximum predicted heart rate, patients were placed inside the magnet bore. Real-time cine of 7 slices without ECG triggering and breath-hold for the functional assessment and perfusion imaging of 3 short-axis slices were acquired. The study protocol was completed with resting perfusion, and late gadolinium enhancement (LGE) imaging was performed to assess myocardial viability. The average time between maximal exercise and start of the imaging was 30±4 seconds, and the duration of the entire study was approximately 1 hour. Cine imaging was completed within 45±4 seconds, and the peak myocardial enhancement during the perfusion imaging was reached within 57±5 seconds of the end of exercise (21). In a recent study conducted by Foster et al., exercise stress CMR was performed with a treadmill constructed of nonferromagnetic components and the hydraulic power system. There was no evidence of attraction of ferromagnetic objects or imaging artifacts, and cine imaging was completed within 40±7 seconds following the termination of exercise (22).

Raman et al. performed treadmill stress CMR and SPECT in ambulatory patients with suspected or known CAD. An imaging protocol included both CMR and SPECT imaging at rest and during the same treadmill exercise test. The average time from the end of exercise to the beginning of imaging was 42.4±5.2 seconds. Cine CMR was performed using the real-time nontriggered bSSFP sequence with parallel imaging and was completed within 68±14 seconds following the termination of exercise. Myocardial perfusion imaging (MPI) was completed in 88±8 seconds. The agreement between SPECT and CMR was moderate (κ=0.58, 95% CI 0.30–0.80). The accuracy to diagnose hemodynamically significant CAD in 8 patients who underwent coronary angiography was 7/8 for CMR and 5/8 for SPECT (P=0.625). There was no incidence of cardiovascular events at the 6-month follow-up in patients with normal findings by either imaging modality (23).

High-Dose Dobutamine Stress Testing

Dobutamine is a synthetic beta 1 selective catecholamine agonist that increases the heart rate, myocardial contractility, and ventricular wall tension. Increased oxygen consumption causes a mismatch between oxygen demand and supply and contraction abnormalities within the myocardial segments supplied by the stenotic coronary artery. The conventional protocol of dobutamine stress CMR (DS-CMR) follows the intravenous administration of dobutamine in incremental doses of 10 μg/(kg·min) every 3 minutes up to a maximum dose of 40 μg/(kg·min) and acquisition of cine loops in the standard views (4-chamber, 2-chamber, 3-chamber, and 3 short-axis cine slices) at rest and each increment of dobutamine dose until the heart rate exceeds 85% of the maximum age-predicted heart rate. For some patients, the additional administration of atropine may be needed to achieve the target heart rate. Because ECG monitoring is limited, an immediate review of acquired cine loops for the development of new wall motion abnormalities is important, and the study must be interrupted in the presence of ischemia and adverse effects or when the target heart rate is achieved (24).

High-dose DS-CMR is a relatively safe and feasible imaging modality. Wahl et al. demonstrated data from 5-year experience in 1000 consecutive patients and reported an overall 6.4% incidence of side effects. There was no death or myocardial infarction, and the rates of major and minor side effects were 0.1% and 6.3%, respectively. Paroxysmal atrial fibrillation was the most frequent cardiac side effect (1.6%) (25). The similar rates of side effects showed Kuijpers et al. in a single center study of 400 consecutive patients. Hypotension (1.5%) and arrhythmias (1.0%) were the most common side effects (26).

DS-CMR is well suited to detect ventricular motion abnormalities in patients with known or suspected CAD. In the study conducted by Pennell et al., 25 patients underwent DS-CMR, dobutamine thallium 201 single-photon emission tomography (DS-SPECT), and quantitative coronary angiography (QCA). The prevalence of hemodynamically relevant CAD was 88%. The majority (91%) of the patients with significant CAD on invasive angiography demonstrated reversible wall motion abnormalities on DS-CMR, and 96% had reversible ischemia on DS-SPECT (27). DS-CMR is an accurate and reliable imaging technique with low interobserver variability for identifying inducible wall motion abnormalities (IWMAs) indicative of a significant coronary lesion (28, 29). DS-CMR at 3 T is feasible and can accurately depict significant CAD with a sensitivity and specificity of 80% and 86%, respectively (30). The diagnostic capability of DS-CMR to detect relevant CAD is similar for both genders (31).

The diagnostic accuracy of DS-CMR has been compared with dobutamine stress echocardiography (DSE) in 208 consecutive patients with suspected CAD. Significant CAD was defined as ⩾50% luminal stenosis and was present in 109 of the 172 patients (64.3%). The image quality of DS-CMR was significantly higher comparing with DSE, and only 3 cases (1.6%) were nondiagnostic. The diagnostic accuracy of DS-CMR was superior to that of DSE (86.0% vs. 72.7%). The sensitivity increased from 74.3% to 86.2% and the specificity from 69.8% to 85.7% for DSE and DS-CMR, respectively (32).

DS-CMR has been shown to be superior to adenosine stress CMR for the detection of IWMAs in patients with suspected or known CAD but without a history of previous myocardial infarction. The dobutamine IWMAs were most accurate to detect coronary stenoses of >50%, while adenosine IWMAs had the highest accuracy to detect >75% luminal narrowing. The sensitivity for the detection of relevant CAD by dobutamine- and adenosine-induced contractility dysfunction and adenosine perfusion imaging were 89%, 40%, and 91% with a specificity of 80%, 96%, and 62%, respectively. Adenosine IWMAs occurred only in the segments with perfusion defects of >75% transmural extent. The visual assessment of adenosine-induced perfusion deficits was sensitive, but less specific (33). The specificities and sensitivities of CMR wall motion imaging studies are summarized in (Table 1).

Gebker et al. investigated the additional role of dobutamine stress perfusion CMR during DS-CMR to detect hemodynamically significant CAD. Perfusion images were acquired at rest and during dobutamine stress in 455 consecutive patients. The addition of perfusion imaging during high-dose DS-CMR for the diagnosis of CAD significantly increased sensitivity, but not specificity. The overall diagnostic accuracy did not change and was 84% (34). The use of new acquisition techniques (strain-encoded CMR) improves the detection of CAD compared with a conventional assessment of regional wall motion on cine images. A cutoff value of the strain rate reserve of 1.64 yielded high accuracy for the depiction of ⩾50% coronary stenosis (P<0.001) (35).

The long-term prognostic value of DS-CMR has also been established. Hundley et al. reported an excellent 2-year cardiac prognosis in patients without inducible ischemia and preserved left ventricular EF (⩾40%), while the evidence of inducible ischemia or reduced left ventricular systolic function (EF<40%) was associated with future myocardial infarction and cardiac death (36). Kuijpers et al. analyzed the prognostic value of DS-CMR in 299 consecutive patients with known or suspected CAD. The cardiac event-free survival rate during a mean follow-up of 24 months was 96.2% in individuals without IWMAs. The patients with negative DS-CMR but rest wall motion abnormalities had a higher annual major adverse cardiac event rate than patients without contractility dysfunction at rest (18% vs. 0.56%) (37).

A prognostic value of adenosine stress perfusion and DS-CMR was investigated in 513 patients with known or suspected CAD and previous myocardial revascularization during a mean follow-up of 2.3 years. An imaging protocol included the first pass of gadolinium diethylene triamine penta-acetic acid (Gd-DTPA) during the infusion of adenosine and high-dose DS-CMR. The 3-year cardiac event-free survival for patients with normal adenosine stress perfusion and without IWMAs during DS-CMR was 99.2%. Inducible ischemia on stress CMR was associated with high risk for future cardiac events (38). In a recent study by Dall'Armellina et al., DS-CMR-induced wall motion abnormalities in individuals with mild-to-moderately reduced left ventricular systolic function (EF 40% to 55%) were associated with a higher risk of future cardiac events and were similar to the risk experienced by individuals with left ventricular EF of <40% with or without an increase in the wall motion score index during DS-CMR (39).

Perfusion Imaging

MPI is performed at rest and during stress induced by an administration of dipyridamole or adenosine by measuring the changes of myocardial signal intensity during the first pass of an intravenously injected bolus of gadolinium-based contrast media. Adenosine is the most often used pharmacological stressor that causes vasodilatation of most vascular beds. Stress agents change the distribution of blood flow within the myocardium supplied by a hemodynamically significant plaque burden with-

Table 1. Sensitivity and Specificity of Cardiovascular Magnetic Resonance Wall Motion Imaging Studies for Detecting Hemodynamically Significant Coronary Stenoses

Study	Magnetic Flux Density, T	No. of Patients	Stressor	Sensitivity, %	Specificity, %
Pennel et al. (27)	1.5	25	Dobutamine	91	100
Van Rugge et al. (28)	1.5	45	Dobutamine	81	100
Nagel et al. (32)	1.5	172	Dobutamine	86	86
Paetsch et al. (33)	1.5	79	Dobutamine	89	80

out a direct impact on the contractile function. The perfusion defect on CMR images appears as a dark area compared with the normally perfused myocardium, which should have a homogeneous gray signal. The diagnostic accuracy of MPI during different cardiac phases is similar (40). The analysis of myocardial perfusion can be done qualitatively, semiquantitatively, or fully quantitatively. Adenosine is usually administered via the peripheral vein at a dosage of 140 $\mu g \cdot kg^{-1} \cdot min^{-1}$. However, in some patients, the standard dose fails to demonstrate a characteristic hemodynamic response. Karamitsos et al. showed that the independent predictors of inadequate response were the age of more than 65 years (P=0.0001) and EF of less than 57% (P=0.0083) and suggested that the high-dose adenosine protocol (up to 210 $\mu g \cdot kg^{-1} \cdot min^{-1}$) could be well tolerated and resulted in an adequate hemodynamic response but with a higher incidence of chest pain in the high-dose group (P=0.009) (41).

Myocardial perfusion reserve after dipyridamole infusion has been used to assess the diagnostic accuracy of perfusion imaging for the detection of relevant CAD and demonstrated significant differences between ischemic and nonischemic myocardial segments. The overall diagnostic sensitivity, specificity, and accuracy for the detection of hemodynamically significant coronary artery stenosis (⩾75%) were 90%, 83%, and 87%, respectively (42). Schwitter et al. compared the capability of first-pass dipyridamole perfusion CMR to detect relevant CAD with positron emission tomography and conventional angiography and reported a sensitivity of 91% and a specificity of 94% for the detection of CAD in comparison with PET, and a sensitivity and specificity of 87% and 85%, respectively, with QCA (43). A semiquantitative assessment of perfusion can be performed by calculating the myocardial perfusion reserve index (MPRI). Nagel et al. achieved a diagnostic accuracy of MPRI of 89% for the detection of significant CAD when 3 inner slices were assessed. The MPRI was calculated from the upslopes of the signal intensity curves at rest and during stress after correction for the upslope of the left ventricular cavity curve (44).

A large meta-analysis reviewed 37 studies (2191 patients) with 24 datasets (1516 patients) using perfusion imaging from multiple centers with a relatively high prevalence of the disease (57%). The analysis of perfusion imaging datasets revealed a sensitivity of 0.91 (95% CI, 0.88 to 0.94) and a specificity of 0.81 (95% CI, 0.77 to 0.85) for the diagnosis of CAD (45). A recent meta-analysis of diagnostic accuracy of stress perfusion CMR for the diagnosis of relevant CAD demonstrated a high sensitivity (89%), but a moderate specificity (80%). Adenosine stress perfusion CMR was more sensitive than dipyridamole stress perfusion CMR (90% vs. 86%, P=0.022), but a difference in specificities was statistically insignificant (81% vs. 77%, P=0.065) (46). CMR perfusion imaging at 3 T provides a higher diagnostic accuracy (90% vs. 82%), sensitivity (98% vs. 90%), specificity (76% vs. 67%), positive predictive value (89% vs. 84%), and negative predictive value (94% vs. 78%) for the detection of significant CAD compared with imagining at 1.5 T (47). The combination of adenosine stress and rest perfusion CMR and delayed enhancement imaging has been shown to be more accurate (88% vs. 68%) to detect hemodynamically relevant CAD (⩾70% luminal obstruction) than perfusion CMR alone (48). The specificities and sensitivities of CMR perfusion studies are shown in Table 2.

A multicenter, multivendor, prospective MR-IMPACT trial compared perfusion CMR with SPECT and concluded that perfusion CMR in the entire study was superior to SPECT and may be considered as an alternative for SPECT imaging in specialized centers. The higher sensitivity and specificity of perfusion CMR is thought to be because of higher spatial resolution (50). A recently published large prospective CE-MARC trial demonstrated the high diagnostic accuracy and superiority of perfusion CMR over SPECT in patients with CAD. The CMR protocol included rest and adenosine stress perfusion, cine imaging, late gadolinium enhancement, and magnetic resonance angiography. Multiparametric CMR provided a higher sensitivity (86.5% vs. 66.5%), specificity (83.4% vs. 82.6%), positive predictive value (77.2% vs. 71.4%), and negative predic-

Table 2. Sensitivity and Specificity of Cardiovascular Magnetic Resonance Perfusion Studies for Detecting Hemodynamically Significant Coronary Stenoses

Study	Magnetic Flux Density, T	No. of Patients	Stressor	Sensitivity, %	Specificity, %
Paetsch et al. (33)	1.5	79	Adenosine	91	62
Al-Saadi et al. (42)	1.5	40	Dipyridamole	90	83
Schwitter et al. (43)	1.5	48	Dipyridamole	87	85
Nagel et al. (44)	1.5	90	Adenosine	88	90
Cheng et al. (47)	1.5	65	Adenosine	90	67
Cheng et al. (47)	3.0	65	Adenosine	98	76
Pilz et al. (48)	1.5	171	Adenosine	96	83
Klem et al. (49)	1.5	100	Adenosine	89	87

tive value (90.5% vs. 79.1%) compared with SPECT. The differences between sensitivities, positive predictive values, and negative predictive values were significant, but between specificities were not (51).

Adenosine stress perfusion CMR can accurately assess the significance of nonculprit vessel ischemia early after successful primary percutaneous intervention (PCI) in patients with acute ST-segment elevation myocardial infarction with the diagnostic accuracy of semiquantitative analysis of 96% (52).

Noninvasive imaging for the assessment of CAD is largely performed by anatomical or functional imaging. Invasively measured fractional flow reserve (FFR) is more reliable for the evaluation of the significance of functional stenosis than noninvasive imaging modalities (53). A recent study compared the accuracy of first-pass adenosine stress perfusion CMR and invasively pressure wire-derived FFR (the value of 0.75 denoted a significant lesion) to detect reversible myocardial ischemia. Of the 76 patients with a perfusion defect on their perfusion images, 97% had an FFR of <0.75 in at least one coronary artery. The overall sensitivity and specificity of first-pass stress perfusion imaging for the detection of functionally significant CAD were 91% and 94%, respectively, with the positive and negative predictive values of 91% and 94%, respectively (54). CMR perfusion imaging at 3 T with new acquisition sequences (k-t SENSE) further improves in-plane resolution (1.2 to 1.2 mm^2) and can be used to detect functionally significant CAD as defined by FFR, using both qualitative and quantitative analyses (55).

First-pass perfusion CMR has a prognostic value and may serve as a reliable tool to reduce the rate of unnecessary invasive coronary angiographies. Pilz et al. reported an excellent 1-year prognosis in patients with normal adenosine stress perfusion imaging and suspected CAD. The major adverse cardiac event rate was 0.92%, and a negative predictive value at 6 and 12 months were 99.5% and 99.1%, respectively (56). Lubbers et al. showed similar results without additional major adverse cardiac events at the 2-year follow-up (57).

A recent study of 158 patients confirmed a very high negative predictive value (96.2%) of normal adenosine stress CMR for relevant CAD. The semiquantitative analysis of CMR perfusion further increased a negative predictive value to 98.7% when using the cutoff values of >1.8 for the arrival time index or 1.2 for the peak time index (58). Furthermore, because of a high negative predictive value, adenosine stress CMR not only reduces the excessive use of invasive angiography but also financial costs (59). Adenosine stress CMR can be used as a noninvasive imaging modality to assess patients with low-risk chest pain at the emergency department (60).

Jahnke et al. evaluated a gender-based prognostic value of combined single session stress CMR in 679 patients during a mean follow-up of 5.3 years and demonstrated equally high predictive power of future cardiac events of adenosine stress perfusion and dobutamine wall motion imaging in individuals with perfusion deficits or wall motion abnormalities. The independent predictors of cardiac events in men were age, diabetes, and the presence of wall motion abnormalities or perfusion defects, while in women, significance predictors were only impaired left ventricular EF (<40%) and the presence of wall motion abnormalities or perfusion detects. Myocardial perfusion and wall motion imaging during stress CMR have similar accuracy to predict cardiovascular events in men and women. The negative combined stress CMR study is associated with the event-free survival of 100% in women for 4 years and >99% in men for 2 years after the CMR examination (61).

The integrated CMR protocol is feasible to detect reversible ischemia in patients who previously were treated by PCI or coronary artery bypass grafting (CABG). The combination of adenosine stress perfusion CMR with late gadolinium enhancement for detecting hemodynamically significant coronary stenosis yielded a sensitivity and specificity of 0.91 and 0.90 in PCI patients, and 0.79 and 0.77 in CABG patients, respectively. Further studies are needed to evaluate how to improve the diagnostic accuracy in patients after surgical revascularization (62).

Dipyridamole and adenosine activate 4 subtypes of the adenosine receptor: A_1, A_{2A}, A_{2B}, and A_3. Coronary vasodilatation is achieved by activating the A_{2A} receptor subtype. However, agents simultaneously stimulate the A_1, A_{2B}, and A_3 subtypes, the activation of which is associated with undesirable adverse effects, such as chest pain, breathlessness, dizziness, nausea, flushing, or atrioventricular (AV) block. Both stress agents can provoke bronchospasm and, therefore, are contraindicated in patients with chronic obstructive lung disease (COPD) and asthma (63–65).

Binodenoson is a highly selective adenosine A_{2A} receptor agonist with a weak affinity for other adenosine receptors. In a study by Udelson et al., pharmacological stress SPECT using 4 different dosing regimens of binodenoson was compared with a standard adenosine SPECT MPI protocol. The investigators demonstrated very good-to-excellent agreement in the extent and severity of reversible perfusion deficits between both stress agents. The frequency of the most common side effects was significantly lower in all dosing regimens of binodenoson compared with those of adenosine ($P \leqslant 0.01$). In the binodenoson group, there was no high-degree AV block, and subjective side effects occurred less frequently and were less severe (66).

Nowadays, only one selective adenosine A_{2A} receptor agonist – regadenoson – is approved for clinical use. Regadenoson has a low affinity for the adenosine A_{2A} receptor subtype, but due to a large receptor reserve in arterial smooth muscle cells, it produces rapid and short maximal coronary vasodilatation. The drug dose is not dependent on patient's weight or renal function (64, 65). The Adenoscan Versus Regadenoson Comparative Evaluation for Myocardial Perfusion Imaging (ADVANCE MPI) 1 and 2 trials demonstrated the noninferiority of regadenoson to adenosine for the detection of reversible perfusion deficits. Regadenoson induced a more rapid and greater increase in the heart rate, but the recovery period was shorter in patients who received adenosine, and no difference in the blood pressure lowering effect was observed. Patients in the regadenoson group developed the most common side effects less frequently, but experienced headache and gastrointestinal discomfort more frequently. Moreover, there was no incidence of third-degree AV block, while first- and second-degree AV block was observed in 2.8% and 0.1% of patients, respectively (67, 68). A recent study by Husain et al. evaluated an immediate and short-term safety profile of regadenoson in patients with COPD and asthma and demonstrated a 0% incidence of clinical exacerbation of the disease and no high-degree AV block (69).

The prognostic significance of ischemic ECG changes during regadenoson stress SPECT in patients without detectable perfusion deficits was investigated by Uthamalingam et al. (70). Stress perfusion SPECT MPI was performed using technetium-99m sestamibi that was injected 30 seconds after the administration of a single 400-μg dose of regadenoson. A 12-lead ECG was recorded before and continuously during the stress test and was assessed every minute. The regadenoson-induced ST-segment depression with normal SPECT-MPI was associated with the annual rate of cardiac death and coronary revascularization of 1.9% and 9.9%, respectively, during the mean follow-up of 14±7 months (70).

Assessment of Myocardial Viability

Left ventricular dysfunction may be a consequence of reversibly or irreversibly injured myocardium. The hibernating myocardium could be described as persistent mechanical dysfunction with reduced coronary flow, but preserved viability (71). The viable myocardium should demonstrate improved contractility in response to pharmacological stress and may recover after successful revascularization, while irreversibly damaged myocytes are replaced by fibrotic tissue and remain dysfunctional despite reperfusion therapy.

Low-Dose Dobutamine Stress

The viable and reversibly dysfunctional myocardium will functionally improve during a low-dose (5–10 $\mu g \cdot kg^{-1} \cdot min^{-1}$) dobutamine infusion. Because of the limited contractile reserve, a further increase in the dobutamine dose results in the worsening of myocardial contractility ("biphasic response"). Baer et al. investigated the capability of low-dose dobutamine stress CMR to detect residual myocardial viability in patients with chronic CAD and compared with 18F-fluorodeoxyglucose positron emission tomography. Dobutamine-induced wall thickening was a better predictor of residual metabolic activity with a higher sensitivity (81% vs. 72%), specificity (95% vs. 89%), and positive predictive value (96% vs. 91%) than end-diastolic wall thickness at rest compared with 18F-fluorodeoxyglucose positron emission tomography (72).

Several studies have demonstrated that the transmural extent of late gadolinium enhancement provides the accurate prognostication of functional recovery after successful revascularization (77, 90). Wellnhofer et al. demonstrated that low-dose dobutamine stress CMR is superior to contrast-enhanced CMR in predicting a functional recovery when the transmurality of myocardial infarction is 1% to 74% (73). Dobutamine-induced systolic wall thickening in patients with chronic left ventricular dysfunction is associated with the transmurality of myocardial scar. The contractile reserve during inotropic stimulation demonstrated dysfunctional segments with the transmural extent of scar tissue of <50% (74). A recent study reported that in patients with a large myocardial scar, the evidence of contractile reserve was a more important predictor for future events than scar tissue (75).

Infarct Imaging

Contrast-enhanced CMR (CE-CMR) is becoming a new first-choice modality for the assessment of myocardial viability. The intravenous injection of a paramagnetic contrast agent significantly improves the diagnostic accuracy of CMR for identifying the extent and distribution of irreversible myocardial injury. The majority of CMR contrast materials approved for clinical use are based on gadolinium chelates. Free gadolinium (Gd^{3+}) ions are toxic; therefore, they must be compounded before administration. Exposure to gadolinium-based contrast media in patients with advanced renal failure has been associated with the development of nephrogenic systemic fibrosis, a potentially fatal disorder. Therefore, the administration of gadolinium-based contrast media is not recommended in the presence of advanced renal failure with an estimated glomerular filtration rate (GFR) of less than 30 mL/(min·1.73 m^2) (76). Gadolinium shortens predomi-

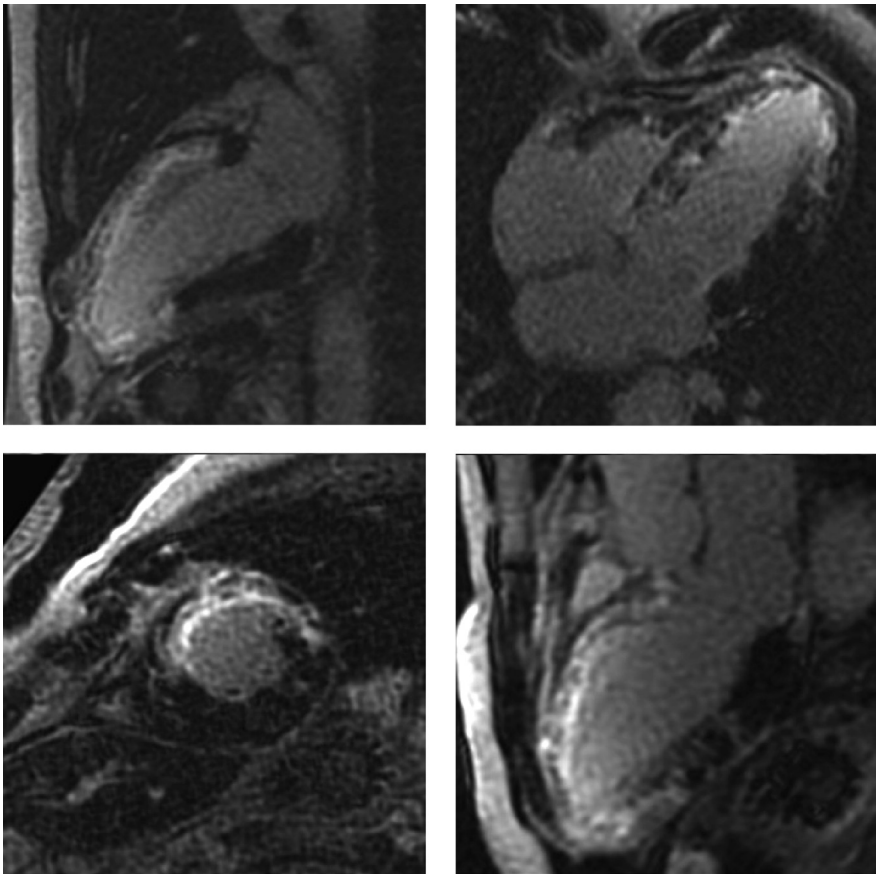


Fig. 3. Long-axis and short-axis contrast-enhanced inversion recovery cardiovascular magnetic resonance images show transmural enhancement in a 71-year-old woman with acute chest pain, ST-segment elevation on ECG, and total occlusion of the proximal left anterior descending coronary artery on conventional angiography

nantly T1 relaxation and increases the signal intensity on T1-weighted images (smaller effect on T2). Images are typically obtained 10 to 20 minutes after the injection of contrast material. This time is optimal to achieve a peak difference between the viable and irreversibly injured myocardium (Fig. 3) (2). The inversion recovery technique increases the signal intensity of infarcted tissue more than 500% by suppressing the signal from the normal myocardium (77).

CE-CMR has been validated as an accurate and reproducible imaging technique to define the infarct size. Kim et al. reported that hyperenhancement was clearly seen after Gd-DTPA administration in both acute and chronic myocardial infarction. The spatial distribution of scar detected by CE-CMR was nearly identical to the necrotic area defined by histopathology at 1 and 3 days or 8 weeks after instrumentation. Conversely, the transient occlusion territory did not enhance despite the presence of myocardial stunning (78). Several studies showed a good correlation with the postmortem data, and there was no significant difference in the infarct size when images were obtained up to 30 minutes after the contrast injection (79). Contrast enhancement in acute injury is visible due to sarcomere rupture and gadolinium diffusion into myocytes (80), while contrast differences at the chronic stage are associated with the presence of fibrotic tissue and delayed wash-in and wash-out kinetics in the infarcted area compared to the normal myocardium (81). Early restoration of blood flow in an occluded coronary artery reduces the transmural extent of hyperenhancement (82). With a high spatial resolution and contrast-to-noise ratio, delayed enhancement imaging can identify subendocardial infarctions undetected by SPECT or PET (83).

The major advantage of CMR over other noninvasive diagnostic modalities is its ability to differentiate between acute and chronic myocardial injury. T2-weighted CMR sequences can determine an increase in the myocardial water content. During an acute stage of myocardial infarction, T2-weighted CMR is able to visualize myocardial edema as the area at risk, which is a feature of acute but not chronic injury. Thus, the combination of late gadolinium enhancement with T2-weighted CMR is a powerful and reliable tool to

differentiate acute from chronic myocardial infarction (84).

PCI-related mild elevations of cardiac biomarkers are common and induced by new myocytes necrosis. Ricciardi et al. found that PCI-related elevations of creatinine kinase-MB were associated with myocardial hyperenhancement within the territory of target vessel perfusion and the mass of infarcted tissue was related to the peak of creatinine kinase-MB level (83).

The benefits of early reperfusion in patients with acute myocardial infarction are well established. However, the ischemic territory may not be properly reperfused despite successful recanalization of an infarct-related artery. CE-CMR is able to detect the extent of microvascular obstruction using the first-pass or early enhancement techniques. The "no-reflow" zones are characterized as the persistent hypointense areas during the first-pass of a contrast agent and are surrounded by the hyperenhanced areas. The region of microvascular obstruction increases up to 48 hours after acute infarction (85) and is associated with a higher risk of cardiovascular complications (86). The presence of microvascular obstruction is associated with a worse functional outcome, larger infarcts, and a greater reduction in the infarct size at follow-up (87).

The transmural extent of hyperenhancement is significantly related to the likelihood of recovery of myocardial contractility after successful revascularization. In a study by Kim et al., myocardial contractility improved in 78% of the segments without hyperenhancement, while only one segment recovered with transmurality of myocardial infarction of >75% (77). The presence of any hyperenhancement detected by CMR is associated with a more than 7-fold increased risk for major adverse cardiac events (88). A recent study demonstrated a linear relationship between transmural viability (<50%), number of viable+normal segments, and the change in left ventricular systolic function in patients with heart failure undergoing CABG (89). The left ventricular end-diastolic wall thickness (EDWT) is associated with the likelihood of functional recovery after revascularization. In a study by Krittayaphong et al., only 9.6% of the segments with an EDWT of <5.5 mm demonstrated an improvement in contractility after revascularization. Late gadolinium enhancement was a better predictor for functional recovery even in patients with an EDWT of <5.5 mm (90).

Myocardial infarctions with atypical or even without symptoms are prevalent among diabetic patients. Kwong et al. investigated 187 diabetic patients with the absence and presence of clinical evidence of myocardial infarction. The presence of delayed enhancement was associated with a more than 3-fold increased risk for major adverse cardiac events and death (HR, 3.71 and 3.61, P=0.001 and P=0.007; respectively) (91). In a large study of CE-CMR with a median follow-up of 4.4 years, Cheong et al. demonstrated that the scar index predicted all-cause mortality or cardiac transplantation in patients with or without CAD. In patients with relatively preserved left ventricular systolic function (EF⩾50%), the presence of delayed enhancement was associated with a worse outcome as compared with the absence of hyperenhancement. Thus, CE-CMR could be a potential noninvasive risk stratification method in patients with preserved left ventricular EF, who may benefit from more aggressive management strategies (92).

Coronary Magnetic Resonance Angiography

Coronary MRA is still limited by low spatial resolution to image coronary arteries small in diameter and long tortuous in their course. A current clinical role of coronary MRA is the detection of anomalous coronary arteries and their anatomical course. However, recent studies report a high sensitivity and specificity of coronary MRA to rule out relevant obstructive CAD (93, 94). Nagata et al. concluded that whole-heart coronary MRA performed at 1.5 T with 32-channel coils might serve as an alternative to multidetector CT coronary angiography in patients who had contraindications to a contrast agent or in young individuals (95). In a recent study, Hamdan et al. concluded that 32-channel 3-T CMR and 64-slice CT coronary angiography similarly identify significant coronary stenosis in patients with suspected or known CAD (96).

Conclusions

Cardiovascular magnetic resonance is one of the newer noninvasive cardiovascular imaging techniques and provides a comprehensive assessment of cardiac anatomy, function, myocardial perfusion and viability in a single study. Recent advances in the magnetic resonance imagining hardware and software improve diagnostic accuracy and make cardiovascular magnetic resonance imaging a possible alternative to the conventional x-ray technique. The use of multiparametric protocols allows a versatile and thorough evaluation of patients with known or suspected coronary artery disease. However, limited availability and costs make cardiovascular magnetic resonance imaging still unachievable to many patients.

Statement of Conflict of Interest

The author state no conflict of interest.

References

1. Natori S, Lai S, Finn JP, Gomes AS, Hundley WG, Jerosch-Herold M, et al. Cardiovascular function in multi-ethnic study of atherosclerosis: normal values by age, sex, and ethnicity. AJR Am J Roentgenol 2006;186: S357-65.
2. Ridgway JP. Cardiovascular magnetic resonance physics for clinicians: part I. J Cardiovasc Magn Reson 2010;12:71.
3. Chuang ML, Hibberd MG, Salton CJ, Beaudin RA, Riley MF, Parker RA, et al. Importance of imaging method over imaging modality in noninvasive determination of left ventricular volumes and ejection fraction: assessment by two- and three-dimensional echocardiography and magnetic resonance imaging. J Am Coll Cardiol 2000;35(2):477-84.
4. Alfakih K, Reid S, Jones T, Sivananthan M. Assessment of ventricular function and mass by cardiac magnetic resonance imaging. Eur Radiol 2004;14(10):1813-22.
5. Kirschbaum SW, Baks T, Gronenschild EH, Aben JP, Weustink AC, Wielopolski PA, et al. Addition of the long-axis information to short-axis contours reduces interstudy variability of left-ventricular analysis in cardiac magnetic resonance studies. Invest Radiol 2008;43(1):1-6.
6. Sechtem U, Pflugfelder PW, Gould RG, Cassidy MM, Higgins CB. Measurement of right and left ventricular volumes in healthy individuals with cine MR imaging. Radiology 1987;163(3):697-702.
7. Semelka RC, Tomei E, Wagner S, Mayo J, Kondo C, Suzuki J, et al. Normal left ventricular dimensions and function: interstudy reproducibility of measurements with cine MR imaging. Radiology 1990;174:763-8.
8. Danilouchkine MG, Westenberg JJ, de Roos A, Reiber JH, Lelieveldt BP. Operator induced variability in cardiovascular MR: left ventricular measurements and their reproducibility. J Cardiovasc Magn Reson 2005;7(2):447-57.
9. Maceira AM, Prasad SK, Khan M, Pennell DJ. Normalized left ventricular systolic and diastolic function by steady state free precession cardiovascular magnetic resonance. J Cardiovasc Magn Reson 2006;8(3):417-26.
10. Karamitsos TD, Hudsmith LE, Selvanayagam JB, Neubauer S, Francis JM. Operator induced variability in left ventricular measurements with cardiovascular magnetic resonance is improved after training. J Cardiovasc Magn Reson 2007;9(5):777-83.
11. Gandy SJ, Waugh SA, Nicholas RS, Simpson HJ, Milne W, Houston JG. Comparison of the reproducibility of quantitative cardiac left ventricular assessments in healthy volunteers using different MRI scanners: a multicenter simulation. J Magn Reson Imaging 2008;28(2):359-65.
12. Bogaert JG, Bosmans HT, Rademakers FE, Bellon EP, Herregods MC, Verschakelen JA, et al. Left ventricular quantification with breath-hold MR imaging: comparison with echocardiography. MAGMA 1995;3(1):5-12.
13. Nowosielski M, Schocke M, Mayr A, Pedarnig K, Klug G, Köhler A, et al. Comparison of wall thickening and ejection fraction by cardiovascular magnetic resonance and echocardiography in acute myocardial infarction. J Cardiovasc Magn Reson 2009;11:22.
14. Mor-Avi V, Jenkins C, Kühl HP, Nesser HJ, Marwick T, Franke A, et al. Real-time 3-dimensional echocardiographic quantification of left ventricular volumes: multicenter study for validation with magnetic resonance imaging and investigation of sources of error. JACC Cardiovasc Imaging 2008;1(4):413-23.
15. Rallidis L, Cokkinos P, Tousoulis D, Nihoyannopoulos P. Comparison of dobutamine and treadmill exercise echocardiography in inducing ischemia in patients with coronary artery disease. J Am Coll Cardiol 1997;30(7):1660-8.
16. Armstrong WF, Zoghbi WA. Stress echocardiography: current methodology and clinical applications. J Am Coll Cardiol 2005;45(11):1739-47.
17. Chow BJ, Beanlands RS, Lee A, DaSilva JN, deKemp RA, Alkahtani A, et al. Treadmill exercise produces larger perfusion defects than dipyridamole stress N-13 ammonia positron emission tomography. J Am Coll Cardiol 2006;47(2): 411-6.
18. American College of Cardiology Foundation Task Force on Expert Consensus Documents, Hundley WG, Bluemke DA, Finn JP, Flamm SD, Fogel MA, Friedrich MG, et al. ACCF/ACR/AHA/NASCI/SCMR 2010 expert consensus document on cardiovascular magnetic resonance: a report of the American College of Cardiology Foundation Task Force on Expert Consensus Documents. J Am Coll Cardiol 2010; 55(23):2614-62.
19. Roest AA, Kunz P, Lamb HJ, Helbing WA, van der Wall EE, de Roos A. Biventricular response to supine physical exercise in young adults assessed with ultrafast magnetic resonance imaging. Am J Cardiol 2001;87(1):601-5.
20. Rerkpattanapipat P, Gandhi SK, Darty SN, Williams RT, Davis AD, Mazur W, et al. Feasibility to detect severe coronary artery stenoses with upright treadmill exercise magnetic resonance imaging. Am J Cardiol 2003;92(5):603-6.
21. Jekic M, Foster EL, Ballinger MR, Raman SV, Simonetti OP. Cardiac function and myocardial perfusion immediately following maximal treadmill exercise inside the MRI room. J Cardiovasc Magn Reson 2008;10:3.
22. Foster EL, Arnold JW, Jekic M, Bender JA, Balasubramanian V, Thavendiranathan P, et al. MR-compatible treadmill for exercise stress cardiac magnetic resonance imaging. Magn Reson Med 2012;67(3):880-9.
23. Raman SV, Dickerson JA, Jekic M, Foster EL, Pennell ML, McCarthy B, et al. Real-time cine and myocardial perfusion with treadmill exercise stress cardiovascular magnetic resonance in patients referred for stress SPECT. J Cardiovasc Magn Reson 2010;12:41.
24. Kramer CM, Barkhausen J, Flamm SD, Kim RJ, Nagel E; Society for Cardiovascular Magnetic Resonance Board of Trustees Task Force on Standardized Protocols. Standardized cardiovascular magnetic resonance (CMR) protocols, society for cardiovascular magnetic resonance: board of trustees task force on standardized protocols. J Cardiovasc Magn Reson 2008;10:35.
25. Wahl A, Paetsch I, Gollesch A, Roethemeyer S, Foell D, Gebker R, et al. Safety and feasibility of high-dose dobutamine-atropine stress cardiovascular magnetic resonance for diagnosis of myocardial ischaemia: experience in 1000 consecutive cases. Eur Heart J 2004;25(14):1230-6.
26. Kuijpers D, Janssen CH, van Dijkman PR, Oudkerk M. Dobutamine stress MRI. Part I. Safety and feasibility of dobutamine cardiovascular magnetic resonance in patients suspected of myocardial ischemia. Eur Radiol 2004;14(10): 1823-8.
27. Pennell DJ, Underwood SR, Manzara CC, Swanton RH, Walker JM, Ell PJ, et al. Magnetic resonance imaging during dobutamine stress in coronary artery disease. Am J Cardiol 1992;70(1):34-40.
28. Van Rugge FP, van der Wall EE, de Roos A, Bruschke AV. Dobutamine stress magnetic resonance imaging for detection of coronary artery disease. J Am Coll Cardiol 1993; 22(2):431-9.
29. Paetsch I, Jahnke C, Ferrari VA, Rademakers FE, Pellikka PA, Hundley WG, et al. Determination of interobserver variability for identifying inducible left ventricular wall motion abnormalities during dobutamine stress magnetic resonance imaging. Eur Heart J 2006;27(12):1459-64.
30. Kelle S, Hamdan A, Schnackenburg B, Köhler U, Klein C, Nagel E, et al. Dobutamine stress cardiovascular magnetic resonance at 3 Tesla. J Cardiovasc Magn Reson 2008;10:44.
31. Gebker R, Jahnke C, Hucko T, Manka R, Mirelis JG, Ham-

dan A, et al. Dobutamine stress magnetic resonance imaging for the detection of coronary artery disease in women. Heart 2010;96(8):616-20.
32. Nagel E, Lehnkuhl HB, Bocksch W, Klein C, Vogel U, Frantz E, et al. Noninvasive diagnosis of ischemia-induced wall motion abnormalities with the use of high-dose dobutamine stress MRI: comparison with dobutamine stress echocardiography. Circulation 1999;99(6):763-70.
33. Paetsch I, Jahnke C, Wahl A, Gebker R, Neuss M, Fleck E, et al. Comparison of dobutamine stress magnetic resonance, adenosine stress magnetic resonance, and adenosine stress magnetic resonance perfusion. Circulation 2004;110(7): 835-42
34. Gebker R, Jahnke C, Manka R, Hamdan A, Schnackenburg B, Fleck E, et al. Additional value of myocardial perfusion imaging during dobutamine stress magnetic resonance for the assessment of coronary artery disease. Circ Cardiovasc Imaging 2008;1(2):122-30.
35. Korosoglou G, Lossnitzer D, Schellberg D, Lewien A, Wochele A, Schaeufele T, et al. Strain-encoded cardiac MRI as an adjunct for dobutamine stress testing: incremental value to conventional wall motion analysis. Circ Cardiovasc Imaging 2009;2(2):132-40.
36. Hundley WG, Morgan TM, Neagle CM, Hamilton CA, Rerkpattanapipat P, Link KM. Magnetic resonance imaging determination of cardiac prognosis. Circulation 2002; 106(18):2328-33.
37. Kuijpers D, van Dijkman PR, Janssen CH, Vliegenthart R, Zijlstra F, Oudkerk M. Dobutamine stress MRI. Part II. Risk stratification with dobutamine cardiovascular magnetic resonance in patients suspected of myocardial ischemia. Eur Radiol 2004;14(11):2046-52.
38. Jahnke C, Nagel E, Gebker R, Kokocinski T, Kelle S, Manka R, et al. Prognostic value of cardiac magnetic resonance stress test: adenosine stress perfusion and dobutamine stress wall motion imaging. Circulation 2007;115(13):1769-76.
39. Dall'Armellina E, Morgan TM, Mandapaka S, Ntim W, Carr JJ, Hamilton CA, et al. Prediction of cardiac events in patients with reduced left ventricular ejection fraction with dobutamine cardiovascular magnetic resonance assessment of wall motion score index. J Am Coll Cardiol 2008; 52(4):279-86.
40. Montwani M, Fairbaim TA, Larghat A, Mather AN, Biglands JD, Radjenovic A, et al. Systolic versus diastolic acquisition in myocardial perfusion MR imaging. Radiology 2012;262(3):816-23.
41. Karamitsos TD, Ntusi NA, Francis JM, Holloway CJ, Myerson SG, Neubauer S. Feasibility and safety of high-dose adenosine perfusion cardiovascular magnetic resonance. J Cardiovasc Magn Reson 2010;12:66.
42. Al-Saadi N, Nagel E, Gross M, Bornstedt A, Schnackenburg B, Klein C, et al. Noninvasive detection of myocardial ischemia from perfusion reserve based on cardiovascular magnetic resonance. Circulation 2000;101(12):1379-83.
43. Schwitter J, Nanz D, Kneifel S, Bertschinger K, Büchi M, Knüsel PR, et al. Assessment of myocardial perfusion in coronary artery disease by magnetic resonance: a comparison with positron emission tomography and coronary angiography. Circulation 2001;103(18):2230-5.
44. Nagel E, Klein C, Paetsch I, Hettwer S, Schnackenburg B, Wegscheider K, et al. Magnetic resonance perfusion measurements for the noninvasive detection of coronary artery disease. Circulation 2003;108(4):432-7.
45. Nandalur KR, Dwamena BA, Choudhri AF, Nandalur MR, Carlos RC. Diagnostic performance of stress cardiac magnetic resonance imaging in the detection of coronary artery disease. J Am Coll Cardiol 2007;50(14):1343-53.
46. Hamon M, Fau G, Née G, Ehtisham J, Morello R, Hamon M. Meta-analysis of the diagnostic performance of stress perfusion cardiovascular magnetic resonance for detection of coronary artery disease. J Cardiovasc Magn Reson 2010; 12(1):29.
47. Cheng AS, Pegg TJ, Karamitsos TD Searle N, Jerosch-Herold M, Choudhury RP, et al. Cardiovascular magnetic resonance perfusion imaging at 3-tesla for the detection of coronary artery disease: a comparison with 1.5-tesla. J Am Coll Cardiol 2007;49(25):2440-9.
48. Pilz G, Bernhardt P, Klos M, Ali E, Wild M, Höfling B. Clinical implication of adenosine-stress cardiac magnetic resonance imaging as potential gatekeeper prior to invasive examination in patients with AHA/ACC class II indication for coronary angiography. Clin Res Cardiol 2006;95(10): 531-8.
49. Klem I, Heitner JF, Shah DJ, Sketch MH Jr, Behar V, Weinsaft J, et al. Improved detection of coronary artery disease by stress perfusion cardiovascular magnetic resonance with the use of delayed enhancement infarction imaging. J Am Coll Cardiol 2006;47(8):1630-8.
50. Schwitter J, Wacker CM, van Rossum AC, Lombardi M, Al-Saadi N, Ahlstrom H, et al. MR-IMPACT: comparison of perfusion-cardiac magnetic resonance with single-photon emission computed tomography for the detection of coronary artery disease in a multicentre, multivendor, randomized trial. Eur Heart J 2008;29(4):480-9.
51. Greenwood JP, Maredia N, Younger JF, Brown JM, Nixon J, Everett CC, et al. Cardiovascular magnetic resonance and single-photon emission computed tomography for diagnosis of coronary heart disease (CE-MARC): a prospective trial. Lancet 2012;379:453-60.
52. Wong DT, Leung MC, Das R, Liew GY, Williams K, Dundon BK, et al. Diagnostic accuracy of adenosine stress cardiovascular magnetic resonance following acute ST-segment elevation myocardial infarction post primary angioplasty. J Cardiovasc Magn Reson 2011;13:62.
53. Pijls NH, De Bruyne B, Peels K, Van Der Voort PH, Bonnier HJ, Bartunek J, et al. Measurement of fractional flow reserve to assess the functional severity of coronary-artery stenoses. N Engl J Med 1996;334(26):1703-8.
54. Watkins S, McGeoch R, Lyne J, Steedman T, Good R, McLaughlin MJ, et al. Validation of magnetic resonance myocardial perfusion imaging with fractional flow reserve for the detection of significant coronary artery disease. Circulation 2009;120(22):2207-13.
55. Lockie T, Ishida M, Perera D, Chiribiri A, De Silva K, Kozerke S, et al. High-resolution magnetic resonance myocardial perfusion imaging at 3.0-Tesla to detect hemodynamically significant coronary stenoses as determined by fractional flow reserve. J Am Coll Cardiol 2011;57(1):70-5.
56. Pilz G, Jeske A, Klos M, Ali E, Hoefling B, Scheck R, et al. Prognostic value of normal adenosine-stress cardiac magnetic resonance imaging. Am J Cardiol 2008;101(10): 1408-12.
57. Lubbers DD, Rijlaarsdam-Hermsen D, Kuijpers D, Kerkhof M, Sijens PE, va Dijkman PR, et al. Performance of adenosine "stress-only" perfusion MRI in patients without a history of myocardial infarction: a clinical outcome study. Int J Cardiovasc Imaging 2012;28(1):109-15.
58. Pilz G, Eierle S, Heer T, Klos M, Ali E, Scheck R, et al. Negative predictive value of normal adenosine-stress cardiac MRI in the assessment of coronary artery disease and correlation with semiquantitative perfusion analysis. J Magn Reson Imaging 2010;32(3):615-21.
59. Pilz G, Patel PA, Fell U, Ladapo JA, Rizzo JA, Fang H, et al. Adenosine-stress cardiac magnetic resonance imaging in suspected coronary artery disease: a net cost analysis and reimbursement implications. Int J Cardiovasc Imaging 2011;27(1):113-21.
60. Lerakis S, McLean DS, Anadiotis AV, Janik M, Oshinski

JN, Alexopoulos N, et al. Prognostic value of adenosine stress cardiovascular magnetic resonance in patients with low-risk chest pain. J Cardiovasc Magn Reson 2009;11:37.
61. Jahnke C, Furundzija V, Gebker R, Manka R, Frick M, Schnackenburg B, et al. Gender-based prognostic value of pharmacological cardiac magnetic resonance stress testing: head-to-head comparison of adenosine perfusion and dobutamine wall motion imaging. Int J Cardiovasc Imaging 2012;28(5):1087-98.
62. Bernhardt P, Spiess J, Levenson B, Pilz G, Höfling B, Hombach V, et al. Combined assessment of myocardial perfusion and late gadolinium enhancement in patients after percutaneous coronary intervention or bypass grafts: a multicenter study of an integrated cardiovascular magnetic resonance protocol. JACC Cardiovasc Imaging 2009;2(11):1292-300.
63. Olah ME, Stiles GL. Adenosine receptor subtypes: characterization and therapeutic regulation. Annu Rev Pharmacol Toxicol 1995;35:581-606.
64. Al Jaroudi W, Iskandrian AE. Regadenoson: a new myocardial stress agent. J Am Coll Cardiol 2009;54(13):1123-30.
65. Johnson SG, Peters S. Advances in pharmacological stress agents: focus on regadenoson. J Nucl Med Technol 2010;38:163-71.
66. Udelson JE, Heller GV, Wackers FJ, Chai A, Hinchman D, Coleman PS, et al. Randomized, controlled dose-ranging study of the selective adenosine A_{2A} receptor agonist binodenoson for pharmacological stress as an adjunct to myocardial perfusion imaging. Circulation 2004;109(4):457-64.
67. Iskandrian AE, Bateman TM, Belardinelli L, Blackburn B, Cerqueira MD, Hendel RC, et al.; ADVANCE MPI Investigators. Adenosine versus regadenoson comparative evaluation in myocardial perfusion imaging: results of the ADVANCE phase 3 multicenter international trial. J Nucl Cardiol 2007;14(5):645-58.
68. Cerqueira MD, Nguyen P, Staehr P, Underwood SR, Iskandrian AE; ADVANCE-MPI Trial Investigators. Effects of age, gender, obesity, and diabetes on the efficacy and safety of the selective A_{2A} agonist regadenoson versus adenosine in myocardial perfusion imaging integrated ADVANCE-MPI trial results. JACC Cardiovasc Imaging 2008;1(3):307-16.
69. Husain Z, Palani G, Cabrera R, Karthikeyan AS, Dhanalakota S, Pathmanathan S, et al. Hemodynamic responce, arrhythmic risk, and overall safety of regadenoson as a pharmacologic stress agent for myocardial perfusion imaging in chronic obstructive pulmonary disease and bronchial asthma patients. Int J Cardiovasc Imaging 2012;28(7):1841-9.
70. Uthamalingam S, Gurm GS, Ahmado I, Sidhu MS, Flynn J. Outcome of patients with regadenoson-induced ST-segment depression but normal perfusion on single-photon emission computed tomography. Angiology 2013;64(1):46-8.
71. Bolli R. Myocardial 'stunning' in man. Circulation 1992;86(6):1671-91.
72. Baer FM, Voth E, Schneider CA, Theissen P, Schicha H, Sechtem U. Comparison of low-dose dobutamine-gradient-echo magnetic resonance imaging and positron emission tomography with [18F]fluorodeoxyglucose in patients with chronic coronary artery disease. A functional and morphological approach to the detection of residual myocardial viability. Circulation 1995;91(4):1006-15.
73. Wellnhofer E, Olariu A, Klein C, Gräfe M, Wahl A, Fleck E, et al. Magnetic resonance low-dose dobutamine test is superior to SCAR quantification for the prediction of functional recovery. Circulation 2004;109(18):2172-4.
74. Rerkpattanapipat P, Little WC, Clark HP, Hamilton CA, Link KM, Hundley WG. Effect of the transmural extent of myocardial scar on left ventricular systolic wall thickening during intravenous dobutamine administration. Am J Cardiol 2005;95(4):495-8.
75. Kelle S, Roes SD, Klein C, Kokocinski T, de Roos A, Fleck E, et al. Prognostic value of myocardial infarct size and contractile reserve using magnetic resonance imaging. J Am Coll Cardiol 2009;54(19):1770-7.
76. Kribben A, Witzke O, Hillen U, Barkhausen J, Daul AE, Erbel R. Nephrogenic systemic fibrosis: pathogenesis, diagnosis, and therapy. J Am Coll Cardiol 2009;53(18):1621-8.
77. Kim RJ, Wu E, Rafael A, Chen EL, Parker MA, Simonetti O, et al. The use of contrast-enhanced magnetic resonance imaging to identify reversible myocardial dysfunction. N Engl J Med 2000;343(20):1445-53.
78. Kim RJ, Fieno DS, Parrish TB, Harris K, Chen EL, Simonetti O, et al. Relationship of MRI delayed contrast enhancement to irreversible injury, infarct age, and contractile function. Circulation 1999;100(19):1992-2002.
79. Amado LC, Gerber BL, Gupta SN, Rettmann DW, Szarf G, Schock R, et al. Accurate and objective infarct sizing by contrast-enhanced magnetic resonance imaging in a canine myocardial infarction model. J Am Coll Cardiol 2004;44(12):2383-9.
80. Jennings RB, Steenbergen C Jr, Kinney RB, Hill ML, Reimer KA. Comparison of the effect of ischaemia and anoxia on the sarcolemma of the dog heart. Eur Heart J 1983;4 Suppl H:123-37.
81. Kim RJ, Chen EL, Lima JA, Judd RM. Myocardial Gd-DTPA kinetics determine MRI contrast enhancement and reflect the extent and severity of myocardial injury after acute reperfused infarction. Circulation 1996;94(12):3318-26.
82. Hillenbrand HB, Kim RJ, Parker MA, Fieno DS, Judd RM. Early assessment of myocardial salvage by contrast-enhanced magnetic resonance imaging. Circulation 2000;102:1678-83.
83. Ricciardi MJ, Wu E, Davidson CJ, Choi KM, Klocke FJ, Bonow RO, et al. Visualization of discrete microinfarction after percutaneous coronary intervention associated with mild creatine kinase-MB elevation. Circulation 2001;103(23):2780-3.
84. Abdel-Aty H, Zagrosek A, Schulz-Menger J, Taylor AJ, Messroghli D, Kumar A, et al. Delayed enhancement and T2-weighted cardiovascular magnetic resonance imaging differentiate acute from chronic myocardial infarction. Circulation 2004;109(20):2411-6.
85. Rochitte CE, Lima JA, Bluemke DA, Reeder SB, McVeigh ER, Furuta T, et al. Magnitude and time course of microvascular obstruction and tissue injury after acute myocardial infarction. Circulation 1998;98:1006-14.
86. Wu KC, Zerhouni EA, Judd RM, Lugo-Olivieri CH, Barouch LA, Schulman SP, et al. Prognostic significance of microvascular obstruction by magnetic resonance imaging in patients with acute myocardial infarction. Circulation 1998;97:765-72.
87. Nijveldt R, Beek AM, Hirsch A, Hofman MB, Umans VA, Algra PR, et al. 'No-reflow' after acute myocardial infarction: direct visualisation of microvascular obstruction by gadolinium-enhanced CMR. Neth Heart J 2008;16:179-81.
88. Kwong RY, Chan AK, Brown KA, Chan CW, Reynolds HG, Tsang S, et al. Impact of unrecognized myocardial scar detected by cardiac magnetic resonance imaging on event-free survival in patients presenting with signs or symptoms of coronary artery disease. Circulation 2006;113(23):2733-43.
89. Pegg TJ, Selvanayagam JB, Jennifer J, Francis JM, Karamitsos TD, Dall'Armellina E, et al. Prediction of global left ventricular functional recovery in patients with heart failure undergoing surgical revascularisation, based on late gadolinium enhancement cardiovascular magnetic resonance. J Cardiovasc Magn Reson 2010;12:56.
90. Krittayaphong R, Laksanabunsong P, Maneesai A, Saiviroonporn P, Udompunturak S, Chaithiraphan V. Compari-

son of cardiovascular magnetic resonance of late gadolinium enhancement and diastolic wall thickness to predict recovery of left ventricular function after coronary artery bypass surgery. J Cardiovasc Magn Reson 2008;10:41.
91. Kwong RY, Sattar H, Wu H, Vorobiof G, Gandla V, Steel K, et al. Incidence and prognostic implications of unrecognized myocardial scar characterized by cardiac magnetic resonance in diabetic patients without clinical evidence of myocardial infarction. Circulation 2008;118(10):1011-20.
92. Cheong BY, Muthupillai R, Wilson JM, Sung A, Huber S, Amin S, et al. Prognostic significance of delayed-enhancement magnetic resonance imaging: survival of 857 patients with and without left ventricular dysfunction. Circulation 2009;120(21):2069-76.
93. Jahnke C, Paetsch I, Schnackenburg B, Bornstedt A, Gebker R, Fleck E, et al. Coronary MR angiography with steady-state free precession: individually adapted breath-hold technique versus free-breathing technique. Radiology 2004;232(3):669-76.
94. Kato S, Kitagawa K, Ishida N, Ishida M, Nagata M, Ichikawa Y, et al. Assessment of coronary artery disease using magnetic resonance coronary angiography: a national multicenter trial. J Am Coll Cardiol 2010;56(12):983-91.
95. Nagata M, Kato S, Kitagawa K, Ishida N, Nakajima H, Nakamori S, et al. Diagnostic accuracy of 1.5-T unenhanced whole-heart coronary MR angiography performed with 32-channel cardiac coils: initial single-center experience. Radiology 2011;259(2):384-92.
96. Hamdan A, Asbach P, Wellnhofer E, Klein C, Gebker R, Kelle S, et al. A prospective study for comparison of MR and CT imaging for detection of coronary artery stenosis. JACC Cardiovasc Imaging 2011;4(1):50-61.

Received 1 March 2013, accepted 30 March 2013